IOP Publishing Plasma Sources Science and Technology

Plasma Sources Sci. Technol. **24** (2015) 065014 (8pp) doi:10.1088/0963-0252/24/6/065014

Complex image method for RF antenna-plasma inductive coupling calculation in planar geometry. Part I: basic concepts

A A Howling[1], Ph Guittienne[2], R Jacquier[1] and I Furno[1]

[1] Ecole Polytechnique Fédérale de Lausanne (EPFL), Swiss Plasma Center, CH-1015 Lausanne, Switzerland

[2] Helyssen, Route de la Louche 31, CH-1092 Belmont-sur-Lausanne, Switzerland

E-mail: alan.howling@epfl.ch

Received 2 June 2015, revised 24 September 2015
Accepted for publication 19 October 2015
Published 6 November 2015

Abstract

The coupling between an inductive source and the plasma determines the power transfer efficiency and the reflected impedance in the primary circuit. Usually, the plasma coupling is analysed by means of a transformer equivalent circuit, where the plasma inductance and resistance are estimated using a global plasma model. This paper shows that, for planar RF antennas, the mutual inductance between the plasma and the primary circuit can be calculated using partial inductances and the complex image method, where the plasma coupling is determined in terms of the plasma skin depth and the distance to the plasma. To introduce the basic concepts, the mutual inductance is calculated here for a linear conductor parallel to the plasma surface. In the accompanying paper part II Guittienne *et al* (2015 *Plasma Sources Sci. Technol.* **24** 065015), impedance measurements on a RF resonant planar plasma source are modeled using an impedance matrix where the plasma-antenna mutual impedances are calculated using the complex image method presented here.

Keywords: complex image method, partial inductance, inductively-coupled plasma, RF antenna

(Some figures may appear in colour only in the online journal)

1. Introduction

For the design and operation of inductively-coupled plasma (ICP) sources, it is important to understand the coupling to the plasma because the plasma loading affects the primary circuit impedance, and therefore the impedance matching and the power transfer efficiency [2]. A model to calculate the source-plasma mutual inductance is useful to optimize ICP source design and for interpretation of experimental measurements.

For simple geometries such as a coil or a solenoid, the self-inductance of an ICP source primary circuit can be calculated using standard formulae [2, 3]. The plasma self-inductance and the source-plasma mutual inductance can also be estimated by making reasonable assumptions about the plasma current geometry. In this way, the electrical properties of an inductive low pressure RF plasma can be analysed by considering the plasma to be a one-turn secondary of an air-core transformer [3]. This *transformer model* [2] is therefore convenient when formulae for the closed current circuit *loop inductances* are known, for example, for coils and solenoids. However, the transformer model approach is problematic in other cases, such as planar RF antennas [4], where the loop inductances of the source and plasma are impractical or impossible to determine using transformer models.

This paper (part I) introduces a complementary approach to calculate the inductive coupling for the case of planar sources and plasmas, based on the *complex image method*. This method gives an intuitive formula for the mutual inductance

between a source current in a straight wire segment and the mirror image current that it induces in a resistive plasma. Arbitrary configurations of planar ICP sources can then be considered by means of a *partial inductance* description [5, 6], whereby a model for the source circuit is first broken down into contiguous linear elements. The source-plasma mutual inductance is finally calculated from the impedance matrix of all the source elements, including their complex image currents in the plasma. Plasma experiments can be interpreted, and future innovative designs could be evaluated, using the understanding gained in this way.

Here in part I, we will concentrate on a single linear current segment above a resistive plasma slab. For a point of comparison with plasma loading, the coupling of a straight wire with the induced current in an ideal screen is first recalled in section 2 using the well-known method of images [7, 8]. The complex image method is then introduced in section 3 to calculate the partial mutual inductance between a wire and the current induced in a resistive plasma slab. Section 4 finally compares the complex image partial inductance approach with the transformer model. The main result is an expression for the complex mutual partial inductance between a linear current source and a resistive plasma slab. This result is exploited in the second paper (part II [1]) to calculate the impedance matrix of a complete network, and to compare theory with plasma experiments using a planar resonant network plasma source.

2. Mutual inductance for a straight wire above an ideal screen

As a preliminary step towards a linear current segment above an infinite plasma half-space, we first consider a straight wire distance h above an infinite, perfectly-conducting ground plane as shown in figure 1. According to the method of images, the magnetic field above the screen, produced by the induced current profile in the screen, is identical to the field produced by an image of the source current reflected in the screen [6, 9]. The image current is in the opposite direction, parallel and at an equal distance h below the screen. For a length of wire which is part of a closed circuit, the mutual inductance between the source current in the wire and the induced current in the ideal screen can be calculated using partial inductances [5, 6]. Since the concept of partial inductance is used here as a tool not commonly used in the plasma literature, the reader is referred to a brief summary of some relevant results in appendix A.

For a straight wire of length l, height h above a perfectly-conducting screen, from (A.6) the mutual partial inductance is

$$M_{\mathrm{p}}^{\mathrm{wire/screen}} \approx \frac{\mu_0}{2\pi} l \left(\ln\left[\frac{l}{h}\right] - 1 \right), \qquad (1)$$

where the approximation is good for $l \gg h$.

The method of images for an ideal screen serves as a reference point for the complex image method in section 3. The concepts of partial inductance will be recalled in section 4 to describe the transformer equivalent circuits for a linear current above an ideal ground screen, and for a linear current above a plasma.

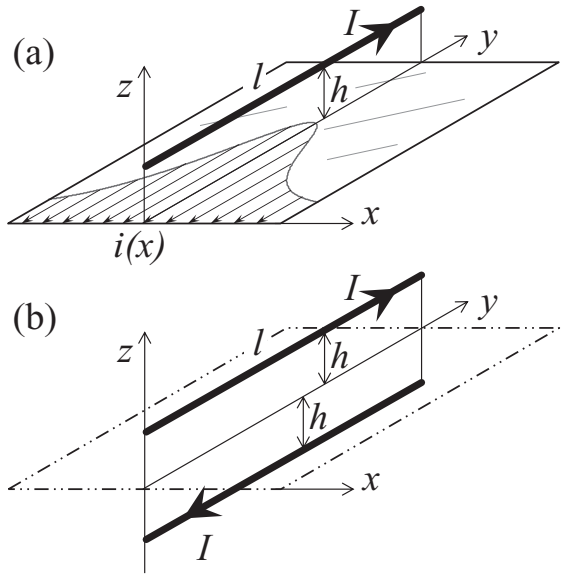

Figure 1. (a) Perspective view of a linear current source element length l, at a distance h above an infinite, perfectly-conducting ground plane. The profile of the induced surface current on the plane is shown schematically. The integral of the current per unit width, $i(x)$, along x is equal and opposite to the source current I. (b) The same source current, with its equal and opposite image current at distance $2h$ below it, to illustrate the method of images.

3. The complex image method applied to resistive plasma

The problem to be solved in this paper is the inductive coupling between a RF current-carrying wire and the current it induces in a resistive plasma. Historically, this problem is analogous to the fundamental studies of resistive-ground return parameters of transmission lines which were motivated by the telecommunications and power industries. Carson [10] developed the most widely accepted approach, where the electromagnetic field due to a line current source above a finitely conducting half-space was expressed as due to the superposition of two sources: the filament current itself, and the induced current flowing in the resistive medium. The results were given in terms of infinite converging Fourier integrals.

It has since been shown [11–20] that the magnetic field above the plane surface of a resistive medium, due to its spatially-distributed induced current, using a two-dimensional quasi-static approximation [18–20] (where displacement currents are neglected), is mathematically equivalent to a real image current filament located at a complex depth in the resistive medium below the line current source; hence the name *complex image method*. It should be understood that the concept of a complex depth is not a physical hypothesis, but a computational convenience [16, 21].

The effective mirroring plane is at a complex distance $\mathbf{p}$ below the medium surface, where $\mathbf{p}$ is the complex skin depth for plane waves, $H = H_0 \mathrm{e}^{-z/\mathbf{p}} \mathrm{e}^{\mathbf{j}\omega t}$. This expression for damped propagating waves is more commonly written as $H = H_0 \mathrm{e}^{-z/\delta} \mathrm{e}^{\mathbf{j}(\omega t - kz)}$, where the (real) skin depth δ is the 1/e distance for field amplitude decay, and k is the wavenumber. The complex skin depth $\mathbf{p}$ is related to δ by [14, 15]

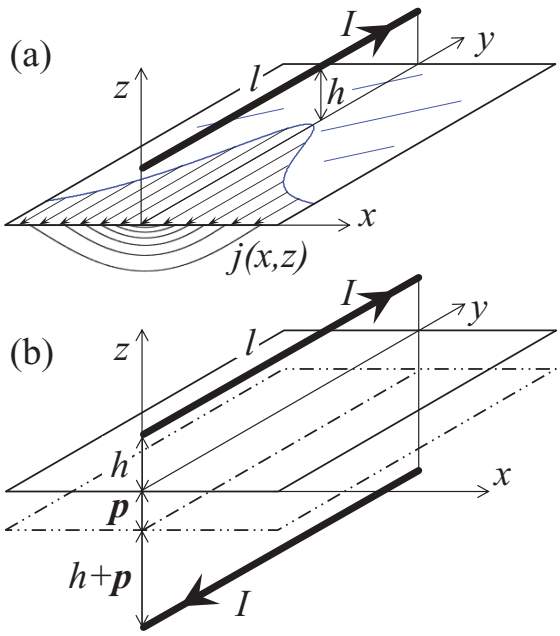

Figure 2. (a) Perspective view of a linear current source element length l, parallel to and at distance h from the surface of a plasma of complex skin depth $\mathbf{p}$. The surface and depth profiles of the induced current in the plasma are shown schematically. The integral of the current density $j(x, z)$ is equal and opposite to the source current I. (b) To illustrate the complex image method, the effective mirror surface is at a complex skin depth distance $\mathbf{p}$ below the plasma surface. Hence the equal and opposite image current is at a complex distance $2(h + \mathbf{p})$ from the current source.

$$\frac{1}{\mathbf{p}} = \sqrt{\mathbf{j}\omega\mu_0\sigma} \qquad \text{and} \qquad \frac{1}{\delta} = \Re\left(\frac{1}{\mathbf{p}}\right), \tag{2}$$

where $\omega = 2\pi f$ with f the alternating current frequency, μ_0 the vacuum permeability, σ the electrical conductivity, and $k = \Im(1/\mathbf{p})$. In a conventional resistive medium where the conductivity is purely real, the skin depth $\delta = (\pi f\mu_0\sigma)^{-1/2}$ and $1/\mathbf{p} = (1 + \mathbf{j})/\delta$.

The distance from source to mirror plane is $(h + \mathbf{p})$, and therefore the image current is a distance $2(h + \mathbf{p})$ from the source [11–20] as shown in figure 2. The spatial distribution of the current penetration into the skin depth is also represented in the figure using a two-dimensional numerical simulation [22] of the electromagnetic fields. Comparison of figure 2 with figure 1 shows that the source-image distance for a resistive medium is $2(h + \mathbf{p})$ instead of $2h$ for a perfectly-conducting screen.

The complex image method has previously been successfully applied to the fields of telecommunications and power transmission [11–16], geophysics [17, 21, 23], and the microelectronics industry [18–20] to obtain solutions for the skin depth effect on inductive coupling in various resistive media. A few papers combine the complex image method with the partial inductance approach; some examples are to be found in the field of microelectronics [18–20]. However, to our knowledge, the complex image method for mutual inductance calculations has not been applied to the field of plasma physics before.

Previous works in complex image theory all consider the resistive medium to have a purely real conductivity, σ. However, electron inertia in a plasma means that the plasma conductivity is complex [2]:

$$\sigma_{\mathbf{pl}} = \frac{\sigma_{\mathrm{dc}}}{1 + \mathbf{j}\omega/\nu_{\mathrm{m}}}, \quad \text{where} \quad \sigma_{\mathrm{dc}} = \frac{n_{\mathrm{e}}q_{\mathrm{e}}^2}{m_{\mathrm{e}}\nu_{\mathrm{m}}}, \tag{3}$$

and q_{e}, m_{e} and n_{e} are respectively the electron charge, mass and number density, ν_{m} the electron-neutral collision frequency, and σ_{dc} the dc conductivity in the limit $\omega \ll \nu_{\mathrm{m}}$. Since the derivation of the complex image theory involves integration in the complex plane [11, 14], it was verified here that the results remain valid when the complex plasma conductivity $\sigma_{\mathbf{pl}}$ is substituted for σ in the expression (2) for the complex skin depth $\mathbf{p}$.

The current image picture can now be used to derive simple formulae for inductances [14, 20] by replacing h in section 2 for the ideal screen, by $(h + \mathbf{p})$. For example, the mutual partial inductance between the wire and its image in the plasma, using (1), is

$$\mathbf{M}_{\mathrm{p}}^{\mathrm{wire/plasma}} \approx \frac{\mu_0}{2\pi} l\left(\ln\left[\frac{l}{(h + \mathbf{p})}\right] - 1\right). \tag{4}$$

Note that h here and in figure 2 is the distance between the wire and the plasma/sheath boundary.

3.1. Assumptions, error evaluation and range of validity

In order to apply the complex image method, the plasma is assumed to be laterally uniform over the length l of the excitation current element. The plasma is also considered to be uniform in depth, for at least a few skin depths from the source conductor where the induced currents are non-negligible, although averaged homogeneous plasma properties can be supposed [14]. If necessary, the complex image method can be extended to treat multiple layers with different properties [14, 19]. The complex image methods above also assume that the plasma fills an infinite half-space, or at least a depth much greater than the plasma skin depth, so that the integrated current profile induced in the plasma is equal and opposite to the source excitation current. Otherwise, for a thin plasma slab or for low plasma density, where the skin depth becomes comparable to, or longer than, the plasma thickness, the complex image method can be adapted using appropriate boundary conditions for the magnetic field at the far side of the plasma [18, 20].

Déri *et al* [14] have compared the exact infinite series results of Carson [10] with the complex image expressions throughout the whole frequency range. It was found that the complex image method is accurate for the limits of large and small values of h/δ, with the largest errors no greater than 10% over an intermediate range $10^{-2} < h/\delta < 10^{0}$. Finally, all transverse dimensions are assumed small compared with the free space wavelength so that a lumped circuit, quasi-static

approximation is valid, and capacitively-coupled displacement currents can be neglected compared to inductively-coupled conduction currents. It should be noted that the quasi-static approximation implies that the complex image model is only valid for RF frequencies much less than the electron plasma frequency ($\omega \ll \omega_{pe}$), because otherwise the displacement current becomes significant [2]. The complex image method is therefore only applicable when the plasma can be described as a resistive conductor rather than as a dielectric medium.

The complex image method therefore gives a good approximation for the magnetic field above a planar plasma using a quasi-static approximation of Maxwell's equations which accounts for the effect of induced currents. However, to the authors' knowledge, it is not known whether the complex image method can be adapted to cylindrical geometry, such as for a solenoid or coil surrounding a plasma column. Such a study is beyond the scope of this paper.

4. Comparison of the transformer model and the complex image method applied to inductively-coupled plasma

The aim of this section is to investigate the equivalence between the transformer model, as commonly used for inductively-coupled plasma sources [2, 3, 24], and the partial inductance treatment of a wire current coupled to a plasma using the complex image method. The partial inductance concept is necessary to separate the total (loop) inductance of a wire/plasma system into primary and secondary transformer circuits coupled by a mutual inductance. The wire/screen system will again be considered first to provide a point of comparison for the wire/plasma system.

4.1. Excitation current in a wire and induced currents in an ideal screen

In figure 3(a), the self partial inductance L_{p11}^{wire} of the wire and its resistance R_1 represent the primary circuit, carrying current I_1, of an equivalent transformer. The self-inductance of the ideal screen, L_{p22}^{screen}, represents the secondary circuit carrying the induced current I_2. Finally, the mutual partial inductance $M_{p12}^{wire/screen}$, from (1), represents the mutual inductance between the primary and secondary circuits. The voltage across the primary circuit is therefore

$$V_1 = R_1 I_1 + \mathbf{j}\omega L_{p11}^{wire} I_1 - \mathbf{j}\omega M_{p12}^{wire/screen} I_2. \tag{5}$$

For the transformer model, the usual next step is to substitute for the current I_2 in terms of I_1 and the estimated impedances in the secondary circuit [2, 3], as resumed in appendix B. However, in the terminology of 'go-and-return circuits' (figure A1) and 'mirror image' methods (figures 1 and 2), it is implicit that the induced current in the secondary circuit here is equal and opposite to the primary circuit source current. Hence $I_1 = I_2$ in figure 3 and (5), respecting the opposite directions of the currents.

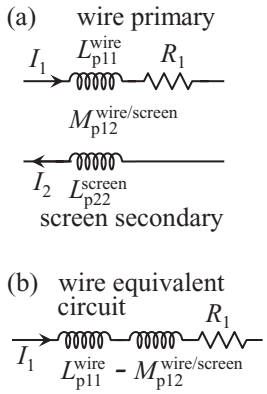

Figure 3. (a) The wire as a primary circuit, and the ideal screen as a secondary circuit, coupled by their mutual inductance. The image current in the screen, I_2, is equal and opposite to the wire current, I_1. (b) The equivalent circuit of the wire, transformed by coupling to the ideal screen.

The impedance V_1/I_1 of the transformed, or coupled, primary circuit in figure 3(b) can therefore be found directly from (5) as

$$\mathbf{Z}_1^{wire/screen} = R_1 + \mathbf{j}\omega(L_{p11}^{wire} - M_{p12}^{wire/screen}). \tag{6}$$

The reflected impedance of the secondary circuit transformed into the primary circuit is therefore equal to the mutual impedance, because the currents in the primary and secondary circuits are equal; this is a consequence of the image description.

4.2. Excitation current in a wire and induced currents in a resistive plasma

By analogy with section 4.1, the impedance of the primary, transformed by inductive coupling to the plasma, is

$$\mathbf{Z}_1^{wire/plasma} = R_1 + \mathbf{j}\omega(L_{p11}^{wire} - \mathbf{M}_{p12}^{wire/plasma}), \tag{7}$$

where the only difference is that the mutual inductance, from (4), is now complex. This wire-to-plasma mutual inductance $\mathbf{M}_{p12}^{wire/plasma}$ represents the effect of plasma coupling on the primary circuit impedance; it is the principal result of this paper, which will be exploited to interpret experimental measurements of a resonant network ICP source in part II [1].

Writing $(h + \mathbf{p})$ as $|h + \mathbf{p}|\exp(\mathbf{j}\varphi)$, the complex mutual inductance in (4) can further be expressed as

$$\mathbf{M}_{p12}^{wire/plasma} \approx \frac{\mu_0}{2\pi} l \left(\ln\left[\frac{l}{|h+\mathbf{p}|} \right] - 1 \right) - \mathbf{j}\frac{\mu_0}{2\pi} l\varphi, \tag{8}$$

where φ is the (negative) argument of $(h + \mathbf{p})$ as shown in figure 5. From (7), the complex mutual impedance in the primary circuit due to plasma coupling, $-\mathbf{j}\omega\mathbf{M}_{p12}^{wire/plasma}$, therefore represents a reduction in real inductance

$$-M_{p12}^{wire/plasma} \approx -\frac{\mu_0}{2\pi} l \left(\ln\left[\frac{l}{|h+\mathbf{p}|} \right] - 1 \right), \tag{9}$$

and an increase in resistance

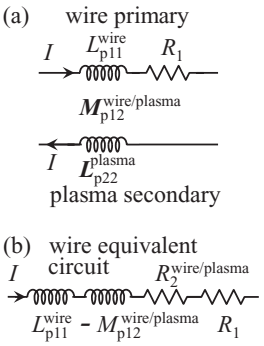

Figure 4. (a) The wire as a primary circuit, and the plasma as a secondary circuit, coupled by their complex mutual inductance. The image current in the plasma is equal and opposite to the wire current. (b) The equivalent circuit of the wire, transformed by coupling to the plasma, which reduces the net inductance (9) and increases its resistance (10).

$$R_2^{\text{wire/plasma}} \approx \frac{\omega\mu_0}{2\pi} l|\varphi|, \tag{10}$$

in the primary circuit as shown in figure 4(b).

For the linear current element considered in this paper (part I), the complex image theory therefore gives an expression (9) for the reduction in ICP source inductance due to currents induced in the plasma, and an expression (10) for the increase in ICP source resistance due to power dissipation coupled into the plasma. Each term depends only on the geometry (length l, and dielectric thickness plus sheath width, h), and the plasma complex skin depth $\mathbf{p}$. The latter is a function of electron density and collision frequency, and the RF excitation frequency. Hence the only plasma parameters necessary to completely determine the inductive plasma coupling are n_e, ν_m, and the effective sheath width. As well as the intuitive picture of image currents for calculating inductances, the complex image method therefore also offers the possibility of a parametric study of plasma coupling to the source, via the simple dependence on plasma complex skin depth $\mathbf{p}$.

4.3. Effect of plasma collisionality

(i) For a fully collisional plasma, $\nu_m \gg \omega$, the plasma conductivity is purely real in (3), as for the conventional resistive medium considered in (2). Hence $\alpha = -\pi/4$ in figure 5 and $-\pi/4 < \varphi < 0$ in (10). The oscillating magnetic field is strongly damped as its power is dissipated in the plasma, with collisional skin depth $\delta_c = (\pi f \mu_0 \sigma_{dc})^{-1/2}$. The ICP source inductance is diminished (9) and its resistance increases (10) due to the inductive plasma coupling.

(ii) For a collisionless plasma, $\nu_m \ll \omega$, the plasma conductivity is purely imaginary in (3). Hence $\mathbf{p}$ is purely real and the magnetic field is evanescent in the plasma with collisionless skin depth $\delta_p = c/\omega_{pe}$, where c is the speed of light in vacuum. The ICP source inductance is still reduced according to (9), but there is no power dissipation in the plasma, hence the ICP source resistance is unchanged by the plasma coupling ($R_2^{\text{wire/plasma}} = 0$ in (10) since $\alpha = \varphi = 0$ in figure 5). However, the effect of stochastic collisions, collisionless heating, and anomalous skin depth could be accounted for by an effective collision frequency [2, 25].

Note that the frequency range of validity is limited by $\omega \ll \omega_{pe}$ because the complex image model assumes that the displacement current is negligible compare to induced conduction current, as mentioned in section 3.1.

(iii) For intermediate collisionality, $\omega \sim \nu_m$, the changes to the ICP source impedance due to plasma coupling can be calculated using (9) and (10).

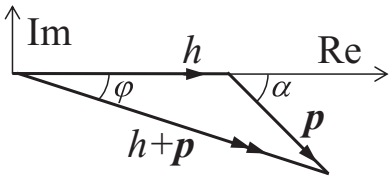

Figure 5. A phasor diagram showing h, the distance to the plasma surface, and $\mathbf{p}$, the plasma complex skin depth. φ is the argument of the resultant ($h + \mathbf{p}$), and α is the phase angle of $\mathbf{p}$.

5. Conclusions

A general method for calculating the inductive coupling to a plasma slab is presented. Firstly, the inductively-coupled plasma source is described using the partial inductance concept, where a model for the primary circuit is broken down into linear contiguous elements. Secondly, the complex image method gives the plasma inductive coupling in terms of the complex mutual partial inductance between the plasma and a linear element. To our knowledge, the complex image method has not previously been applied to plasma physics in this context. Simple expressions are given for the change in inductance and resistance of the ICP source due to plasma loading. The plasma coupling is determined by the plasma complex skin depth, and the distance between the source element and the plasma. The complex image method, combined with the partial inductance approach, can be used to estimate the plasma loading for planar plasma source geometries.

These results are used in a second paper, part II [1], to calculate the impedance matrix of a complete inductively-coupled source, and to compare the theory with plasma experiments using a planar resonant network antenna.

Acknowledgments

We thank Dr Ch Hollenstein for many useful comments, and Drs J Larrieu and P Fayet of Tetra Pak SA, Romont, Switzerland, for their advice and support. The development of a plasma source was supported by the Swiss Commission for Technology and Innovation grant no. CTI 14693.1 PFIW-IW.

Appendix A. Partial inductance

A brief description of partial inductances is presented here as a necessary step to define and calculate the self partial inductance and mutual partial inductance between parallel current filaments. These results also apply directly to plasma coupling calculations for an antenna network made up of orthogonal straight sections in part II [1]. A full account of the partial inductance concept is given by Ruehli [5], and the recent book by Paul [6] is dedicated to loop and partial inductances.

There are two fundamental approaches to inductance calculations: the most common approach is to calculate the *loop inductance* from the magnetic flux linking a closed current circuit [6]. This is convenient when the circuit geometry is sufficiently simple and well-defined for the magnetic flux to be calculated, such as for a coil or a solenoid. However, when the current path is difficult to define, or when various parts of the circuit are coupled to different current circuits, it is not possible to calculate a unique loop inductance.

Alternatively, the *partial inductances* [6] of all the contiguous partial elements of a closed circuit can be calculated and combined in an impedance matrix, which includes all the mutual inductances, to give the complete circuit inductance. These two different methods date from the origins of electromagnetic theory (for a review see [26]) up to modern works [6].

A.1. Partial inductances for straight wire segments

The *self partial inductance* of one linear element of a current circuit is defined as the magnetic flux ψ_p, per unit current, between the current segment and infinity,

$$\psi_\mathrm{p} = \int_{r=a}^{\infty}\int_{z=-l/2}^{l/2} B\,\mathrm{d}z\,\mathrm{d}r, \tag{A.1}$$

where the magnetic field B, using the Biot-Savart law, is [6, 27],

$$B = \frac{\mu_0 I}{4\pi}\int_{z=-l/2}^{l/2}\frac{\sin\theta}{R^2}\,\mathrm{d}z, \tag{A.2}$$

and I is the current in the wire. By integration, the self partial inductance of a straight cylindrical wire of radius a and length l is approximately [6, 27, 28]

$$L_\mathrm{p}^\mathrm{wire} \approx \frac{\mu_0}{2\pi} l\left(\ln\left[\frac{2l}{a}\right] - 1\right), \tag{A.3}$$

where the approximation is good for $l \gg a$. This is implicitly the *external* self partial inductance because current flows only in the surface of the wire due to the skin effect in metals at radio frequencies; there is therefore no internal magnetic flux in the wire.

The *mutual partial inductance*, M_p, between two segments is the magnetic flux, due to unit current in the first segment, between the second segment and infinity [6]. For wires of length l, separation $2h$, it is obtained by replacing the wire radius a in (A.3) by the new effective radius $2h$ to obtain [6, 27, 28]

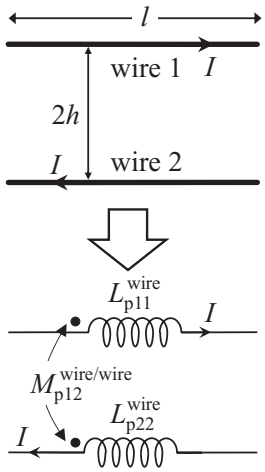

Figure A1. Model of a two-wire return circuit of parallel conductors in terms of partial inductances [6].

$$M_\mathrm{p}^\mathrm{wire/wire} \approx \frac{\mu_0}{2\pi} l\left(\ln\left[\frac{l}{h}\right] - 1\right), \tag{A.4}$$

where the approximation is good for $l \gg h \gg a$. This approximation will be appropriate here for comparison with the loop inductance, although more exact expressions will be used in the following paper, part II [1]. Formal proofs of partial inductances for arbitrary orientations of current segments are given in references [5] and [6], but the simplest case of parallel current filaments is sufficient to calculate the total inductance of an antenna network made up of straight wires in part II [1].

Figure A1 shows a two-wire transmission line for a go-and-return current circuit made up of two of these wires. The *net partial inductance* [6] (alternatively called the *effective partial inductance* or simply the *partial inductance*) of wire 1 is defined as $L_1 = L_{\mathrm{p11}}^{\mathrm{wire}} - M_{\mathrm{p12}}^{\mathrm{wire/wire}}$, and similarly for wire 2. The total, or loop, inductance of this section of transmission line is obtained by summing the flux contributions of all the partial inductances:

$$L_\mathrm{loop}^\mathrm{wire/wire} = L_{\mathrm{p11}}^{\mathrm{wire}} + L_{\mathrm{p22}}^{\mathrm{wire}} - 2M_{\mathrm{p12}}^{\mathrm{wire/wire}} \approx \frac{\mu_0}{\pi} l \ln\left[\frac{2h}{a}\right], \tag{A.5}$$

where the mutual inductance contributions are subtracted because the currents are in opposite directions [6, 27, 28]. The partial inductance method therefore gives the same result as in standard textbooks for the loop inductance of a two-wire transmission line of length l, separation distance $2h$, when proximity and end effects are neglected.

A.2. Partial inductances for a straight wire segment above an ideal screen

According to the well-known method of images [7, 8], the field produced by the current profile induced on the screen is identical to the field produced by the image of the original current reflected in the screen [6, 9]. The image current is therefore parallel and opposite at an equal distance h below the screen.

Because the magnetic field above the plane remains the same as for the two-wire system, the results of the two-wire transmission line can be directly applied. The self partial inductance L_{p11}^{wire} of the wire is therefore the same as (A.3), and the mutual partial inductance of the wire and the screen is also unchanged with regard to (A.4):

$$M_{p}^{wire/screen} \approx \frac{\mu_0}{2\pi} l \left(\ln \left[\frac{l}{h} \right] - 1 \right). \tag{A.6}$$

However, the magnetic field exists only in the upper half-space and so the loop inductance is one half of the two-wire system in (A.5):

$$L_{loop}^{wire/screen} \approx \frac{\mu_0}{2\pi} l \ln \left[\frac{2h}{a} \right], \tag{A.7}$$

which, again, is the same result as in standard textbooks for the inductance of a wire-to-plane transmission line of length l, when proximity and end effects are neglected [6].

The net partial inductance of the wire, $L_1 = L_{p11}^{wire} - M_{p12}^{wire/image}$, is now equal to the total (loop) inductance, which implies that the net partial inductance of the idealized ground plane is zero [29]. This is self-consistent with the concept of a perfect magnetic screen, because the magnetic flux due to the current induced in the screen self partial inductance exactly cancels the flux associated with the mutual partial inductance due to the current in the wire. We also note that expressions for the net partial inductance of a finite screen tend to zero as the plane width tends to infinity [29, 30]. Furthermore, a zero net partial inductance also means that the voltage drop along a perfect ground plane is zero (no fields beyond a perfect screen).

Appendix B. Brief summary of the transformer method

In figure B1, the ICP source is a primary circuit with current I_1, voltage V_1, resistance R_1 and loop self-inductance L_{11}. The plasma current I_2 is effectively a single-turn air-cored secondary circuit with loop self-inductance L_{22} determined by the geometry of the plasma current path. This current path has plasma impedance $\mathbf{Z}_{pl} = R_2(1 + \mathbf{j}\omega/\nu_m)$, where R_2 is the plasma current path resistance, and $\mathbf{j}R_2\omega/\nu_m$ is the inductance due to electron inertia which follows from the plasma complex conductivity in (3) [2, 3]. The mutual loop inductance between the primary and secondary loop inductances is M_{12}. Applying Kirchoff's law to the primary and secondary circuits gives

$$V_1 = R_1 I_1 + \mathbf{j}\omega L_{11} I_1 - \mathbf{j}\omega M_{12} I_2, \tag{B.1}$$

$$0 = \mathbf{Z}_{pl} I_2 + \mathbf{j}\omega L_{22} I_2 - \mathbf{j}\omega M_{12} I_1. \tag{B.2}$$

Substituting for I_2 from (B.2) in (B.1) gives the primary impedance $\mathbf{Z}_1 = V_1/I_1$ as follows:

$$\mathbf{Z}_1 = R_1 + \mathbf{j}\omega L_{11} + \frac{\omega^2 M_{12}^2}{(\mathbf{Z}_{pl} + \mathbf{j}\omega L_{22})}, \tag{B.3}$$

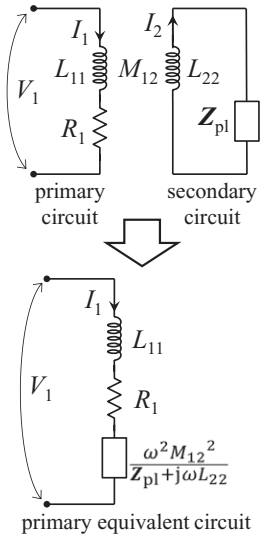

Figure B1. The electrical circuit of an ICP source (primary circuit) and an inductive plasma (secondary circuit), with the equivalent circuit of the primary, transformed by inductive coupling to the plasma.

where $(\mathbf{Z}_{pl} + \mathbf{j}\omega L_{22})$ is the secondary circuit impedance. In figure B1, the secondary circuit impedance has been transformed into its series equivalent impedance in terms of the primary circuit current.

References

[1] Guittienne P, Jacquier R, Howling A A and Furno I 2015 *Plasma Sources Sci. Technol.* (part 2) **24** 065015
[2] Lieberman M A and Lichtenberg A J 2005 *Principles of Plasma Discharges and Materials Processing* 2nd edn (New York: Wiley)
[3] Piejak R B, Godyak V A and Alexandrovich B M 1992 *Plasma Sources Sci. Technol.* **1** 179
[4] Guittienne P, Lecoultre S, Fayet P, Larrieu J, Howling A A and Hollenstein C 2012 *J. Appl. Phys.* **111** 083305
[5] Ruehli A E 1972 *IBM J. Res. Dev.* **September 1972** 470
[6] Paul C R 2010 *Inductance: Loop and Partial* (New York: Wiley)
[7] Harrington R F 1958 *Introduction to Electromagnetic Engineering* (New York: McGraw-Hill)
[8] Smythe W R 1968 *Static and Dynamic Electricity* 3rd edn (New York: McGraw-Hill)
[9] Paul C R 2006 *Introduction to Electromagnetic Compatibility* 2nd edn (New York: Wiley)
[10] Carson J R 1926 *Bell Syst. Tech. J.* **5** 539
[11] Wait J R 1961 *Proc. IRE* **49** 1576
[12] Wait J R and Spies K P 1969 *Can. J. Phys.* **47** 2731
[13] Bannister P R 1970 *Radio Sci.* **5** 1375
[14] Déri A, Tevan G, Semlyen A and Castanheira A 1981 *IEEE Trans. Power Appar. Syst.* **PAS-100** 3686
[15] Déri A and Tevan G 1981 *Archiv Elektrotechnik* **63** 191
[16] Bannister P R 1986 *Radio Sci.* **21** 605
[17] Boteler D H and Pirjola R J 1998 *Geophys. J. Int.* **132** 31
[18] Weisshaar A, Lan H and Luoh A 2002 *IEEE Trans. Adv. Packag.* **25** 288
[19] Jiang R, Fu W and Chen C C P 2005 *IEEE Trans. Comput.—Aided Des. Integr. Circuits Syst.* **24** 1562
[20] Kang K, Shi J, Yin W Y, Li L W, Zouhdi S, Rustagi S C and Mouthaan K 2007 *IEEE Trans. Magn.* **43** 3243
[21] Park D 1973 *J. Geophys. Res.* **78** 3040

[22] COMSOL Inc. www.comsol.com
[23] Thomson D J and Weaver J T 1975 *J. Geophys. Res.* **80** 123
[24] Gudmundsson J T and Lieberman M A 1998 *Plasma Sources Sci. Technol.* **7** 83
[25] Lieberman M A and Godyak V A 1998 *IEEE Trans. Plasma Sci.* **26** 955
[26] Leferink F B J 1995 *IEEE Int. Symp. Electromagnetic Compatibility* (*Atlanta, GA, USA*, *14–18 August 1995*) p16
[27] Rosa E B 1907 *Bull. Natl Bur. Stand.* **80** 301
[28] Grover F W 1962 *Inductance Calculations: Working Formulas and Tables* (New York: Dover)
[29] Hockanson D M, Drewniak J L, Hubing T H, Doren T P V, Sha F, Lam C W and Rubin L 1997 *IEEE Trans. Electromagn. Compat.* **39** 286
[30] Holloway C L and Kuester E F 1998 *IEEE Trans. Electromagn. Compat.* **40** 33